Renewable and Sustainable Energy Reviews 127 (2020) 109888

Contents lists available at ScienceDirect

Renewable and Sustainable Energy Reviews

journal homepage: http://www.elsevier.com/locate/rser

A methodology for reliability assessment and prognosis of bearing axial cracking in wind turbine gearboxes

Yi Guo *, Shuangwen Sheng, Caleb Phillips, Jonathan Keller, Paul Veers, Lindy Williams

National Renewable Energy Laboratory, Golden, CO, 80401, United States

ARTICLE INFO

Keywords:
Wind turbine
Reliability assessment
Prognosis
Axial cracking
Probability of failure
Gearbox

ABSTRACT

This article describes an interdisciplinary methodology to calculate the probability of failure for bearing axial cracking, the dominant failure mode in the intermediate and high-speed stages of many wind turbine gearboxes. This approach is mainly a physics-domain method with needed inputs from the data domain. The gearbox and bearing design along with operations data and component failure records from a wind power plant provide the input to physics-based models and define axial cracking damage metrics. The physics-domain models predict the bearing loads and sliding velocities, which are the essential elements for quantifying the accumulated frictional energy. Both accumulated frictional energy and electrical energy generation are proposed as damage metrics for bearing axial cracking. A first-order reliability method is then used to compare the proposed damage metrics to failure threshold functions and calculate the probability of failure of each individual bearing. Although the probability of failure for the failed turbines is not separated from the population, a feature engineering analysis shows the potential of frictional energy as a damage metric when combined with roller loads, bearing sliding speed, lubricant type, and terrain features. Through statistical analysis of historical data, the proposed methodology enables reliability assessment of axial cracking in individual wind turbine bearings and connects the reliability forecast with turbine design and operations.

1. Introduction

Wind power plant operation and maintenance (O&M) costs can be as high as 30% of the life-cycle cost of a typical offshore wind plant, and about half of that for a typical land-based wind plant [1]. Premature failures of wind turbine drivetrain components remain an important contributor to higher-than-expected O&M costs of wind power plants [2]. An accurate reliability forecast provides crucial information for reducing O&M costs through design improvements, optimized operation strategies, and enhanced budgeting.

The current research focuses on reliability modeling and prognosis by examining bearing axial cracking, which is the dominant failure mode observed in the high- and intermediate-speed-stage bearings in many wind turbine gearboxes [3]. "Axial" describes the orientation of these cracks, as they align with the axis of the shaft rotation. These cracks typically have white etching areas, which are also referred as white etching cracks (WECs). "White etching" refers to the appearance of the steel microstructure when the cracked bearing cross sections are polished, etched with chemicals, and examined under reflected light [4]. These cracks tend to propagate to spalls or lead to a complete splitting of the bearing inner ring. This mode of failure can occur at 5%–20% of the predicted design life based on rolling contact fatigue and has been observed in many industries, bearing locations, bearing types, bearing parts, and steel types [5,6]. Although WECs have been reported for over a decade, the conditions leading to axial cracking or WECs, the process by which this failure culminates, and the reasons for their apparent prevalence in wind turbine gearboxes, are all highly debated. In 2014, benchtop testing conducted at Argonne National Laboratory reproduced WECs on a three-ring-on-roller test rig under highly loaded sliding conditions [7]. A cumulative frictional-energy metric was derived from the benchtop testing results [8] for identifying the occurrence of axial cracking. Based on this damage metric, the presented research aims to introduce and demonstrate a reliability assessment methodology for axial cracking.

Component reliability is typically assessed by fitting the component age at the time of failure with a mathematical distribution, such as Weibull. This data-domain method provides a quantitative approach to compare various designs, manufacturers, operations, and maintenance [9]. It has been successfully applied in military, civil, and many other

* Corresponding author.
E-mail addresses: yi.guo@nrel.gov (Y. Guo), shuangwen.sheng@nrel.gov (S. Sheng), caleb.phillips@nrel.gov (C. Phillips), jonathan.keller@nrel.gov (J. Keller), paul.veers@nrel.gov (P. Veers), lindy.williams@nrel.gov (L. Williams).

https://doi.org/10.1016/j.rser.2020.109888
Received 30 July 2019; Received in revised form 6 April 2020; Accepted 27 April 2020
Available online 8 May 2020
1364-0321/

Nomenclature

T	Main shaft torque (*Nm*)
ω_g	Generator rotational speed (*rpm*)
E	Frictional energy (*J*)
$\hat{E}$	Frictional energy (nondimensional)
$\hat{E}^{\star}$	Frictional energy threshold (nondimensional)
G	Limit state function
P_f	Probability of failure
T_h	High-speed-shaft torque (*Nm*)
ε	Gearbox ratio
η_g	Transmission efficiency
M	Mass matrix (*kg*)
C	Damping matrix (Ns/m)
K	Stiffness matrix (N/m)
m_b	Mass of the brake disc (*kg*)
m_{sh}	Mass of the shaft (*kg*)
q	Displacement vector (*m*)
t	Time (*s*)
f	External load (*N*)
ξ	Damping ratio
ω_n	Natural frequency (*Hz*)
U	Mode shape matrix (*m*)
N	Number of bins
μ	Frictional coefficient
Q_{ij}	Normal force between inner raceway and roller *j* (*N*)
ΔV_{ij}	Sliding velocity (m/s)
ω_c	Bearing cage rotational speed (*rpm*)
ω_{rj}	Roller *j* rotational speed (*rpm*)
B	Bearing inner ring raceway diameter (*mm*)
d_m	Bearing pitch diameter (*mm*)
D	Roller diameter (*mm*)
Z	Number of rollers
L	Roller length (*mm*)
C_{ij}	Contact load factor
b_{ij}	Length of contact ellipse (*mm*)
F_R	Bearing radial load (*N*)
β	Weibull shape parameter
η	Weibull scale parameter
γ	Weibull location parameter
ΔP_d	Bearing clearance variation (*mm*)
Γ	Coefficient of expansion
T_o	Bearing outer ring temperature (°*C*)
T_i	Bearing inner ring temperature (°*C*)
T_a	Ambient temperature (°*C*)
Ψ	Probability density function
Φ	Cumulative distribution function
d_o	Bearing outer ring raceway diameter (*mm*)
d_i	Bearing inner ring raceway diameter (*mm*)
R	Reliability index
PH	Electrical energy generation (*MWh*)
$PH^{\star}$	Electrical energy generation threshold (*MWh*)

Abbreviations

O&M	Operation and maintenance
WEC	White-etching crack
SCADA	Supervisory control and data acquisition
HSS	High-speed shaft
HSB	High-speed-shaft bearings
RS	Rotor side
GS-in	Generator-side inboard

applications [10] and received attention in the wind industry, especially for plant or fleetwide reliability analysis [11]. However, these reliability analyses are conducted at the wind plant or fleet levels, and they do not provide much information on individual turbines and their subcomponents.

During wind plant operations, a large amount of turbine supervisory control and data acquisition (SCADA), condition monitoring, and plant maintenance records are typically collected. Various modeling and analysis methods using the collected data have been explored for condition-based maintenance of major turbine components [12]. However, the focus has been on fault diagnostics but not prognostics. Prognostic methods for wind are still being explored [13] and they can be grouped into physics-based, statistical, artificial intelligence, and hybrid approaches [14,15]. Statistical, artificial intelligence, and reliability engineering life data analysis can be broadly considered as data-driven approaches. These data-domain-reliability prediction methods are highly influenced by the availability of high-quality, informative turbine component reliability data. Most importantly, these approaches are not capable of connecting reliability estimates with component design parameters, operation strategies, and control objectives because of the lack of physical understanding of underlying failure mechanisms. In other words, methodologies for addressing reliability evaluation throughout a component's life cycle, including its initial design phases and various operational conditions, are yet to be developed.

In this work, a novel interdisciplinary methodology that uses information from both the physics and data domains is developed for both reliability assessment and prognosis of wind turbine gearbox bearing axial cracking. The statistical characteristics of bearing damage and failure for a wind plant are assessed by analyzing the accumulated frictional energy of individual turbine bearings using historical SCADA data and failure records. Assuming the rest of the wind plant has the same frictional energy failure threshold as the failed turbines, reliability forecast of individual bearings at any operating age is estimated. Moreover, reliability forecast of wind turbine gearbox bearings inherently considers the effects of bearing design and turbine operations because of the physical nature of this methodology, which can be used in early design phases to forecast and reduce O&M costs.

This methodology includes a set of mathematical models together with operation data and component failure records to calculate probability of failure of gearbox bearings of individual wind turbines throughout the turbines entire life cycle. Bearing accumulated frictional energy and electrical power generation are considered as damage metrics for axial cracking in this study. The reliability assessment using accumulated frictional energy includes the following steps: 1) mapping turbine rotor loads to drivetrain loads, 2) calculating bearing roller sliding, 3) estimating the progression of bearing damage, and 4) assessing probability of failure considering uncertainties in modeling parameters and input signals. Similarly, reliability assessment of bearing axial cracking using electrical power generation includes: 1) calculating the accumulation of electrical power for individual turbines, 2) determining bearing degradation, and 3) assessing probability of failure. The input for these models comprises wind plant SCADA data, maintenance records, and basic drivetrain design parameters and dimensions. The bearing degradation is determined using the aforementioned metrics and the degradation threshold is calculated using the failure and maintenance records from wind power plants. Bearing degradation and probability of failure is evaluated for forty-nine MW-size wind turbines of a wind plant. With this methodology, many other damage metrics, failure modes, or drivetrain components can be easily examined.

The rest of the article is organized as follows. Section 2 introduces

the reliability modeling and prognosis methodology. It first illustrates the flow of the methodology and then briefly discusses various models developed from loads to probability of failure. Section 3 presents results of the methodology using data from an actual wind plant and discusses a correlation between various features and component probability of failure prediction. Then, the component probability of failure evaluation is presented based on the frictional energy accumulation induced by roller sliding. Finally, the electrical energy produced is considered as an alternative metric and compared to the frictional energy approach. This article concludes with a summary of the current research and a brief discussion of future work.

2. Methodology

This section describes the probability of failure calculation method using a set of mathematical models and wind power plant SCADA data. The developed models are analytic and therefore can be applied to wind plants with various drivetrain configurations or designs. Steps for calculating the bearing frictional energy and probability of failure of individual turbines within the wind plant are illustrated in Fig. 1 and Fig. 2, respectively.

As shown in Fig. 1, the power, gearbox lubricant temperature, and rotor speed are taken directly from the turbine SCADA data. Main shaft torque, T in Nm, is not directly measured but can be estimated using measured electrical power and generator speed.

The lumped-parameter gearbox model calculates gearbox bearing radial loads and displacements at any given torque. The loads on individual bearing rollers are then estimated [19]. Considering roller loads, bearing rotational speed, and lubricant temperature, an analytic roller dynamics model then computes the roller sliding speeds. Given roller sliding speed and roller loads, $\widehat{E}$ is the summation of the nondimensonal energy between each roller as it orbits the inner raceway. Frictional energy generated at the interface between the rollers and cage is not considered because axial cracking appears on the bearing raceways, not the rollers.

By following the same steps described in Fig. 1, the frictional energy accumulation can be estimated for all the turbines within the plant. Combining information on frictional energy accumulation for both healthy and failed turbines based on the plant failure records, the Weibull distribution of the damage threshold $\widehat{E}^{\star}$ of the accumulated frictional energy is determined statistically as illustrated in Fig. 2. Given the significant uncertainties in calculating $\widehat{E}^{\star}$, its Weibull distribution is used instead of a constant value. A limit state function G is then defined that separates healthy and failure domains by subtracting the frictional energy threshold from energy accumulation for a given operating period of an individual wind turbine. Finally, a reliability analysis approach called first order reliability method (FORM) [16,17] is applied to calculate probability of failure P_f of individual turbine bearings considering the variability in lubricant temperature, bearing clearance,

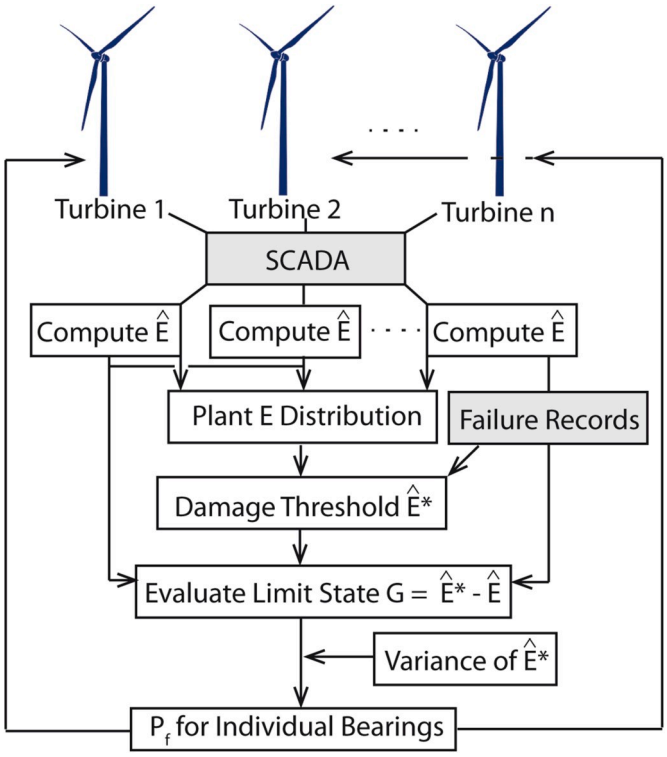

Fig. 2. Modeling steps for calculating the probability of failure (P_f) of individual bearings.

and frictional energy threshold. Depending on the specified temperature, speed and torque spectra for the analysis, P_f of individual turbines bearings can be assessed for a given time in the past or forecasted for the future. In the next section, these mathematical models are detailed.

2.1. Gearbox model

There are two cylindrical bearings supporting the high-speed shaft (HSS) of the studied gearboxes. One of them is mounted close to the rotor-side end of the shaft (RS), whereas the other is located near the generator (GS-in). To calculate the bearing loads, a three-degree-of-freedom lumped-parameter model is established. This lumped-parameter model uses torque as the input and calculates the radial loads and displacements of all three bearings mounted on the high-speed shaft. HSS torque in the gearbox can be calculated using $T_h = \frac{T}{\varepsilon}\eta_g$, where ε and η_g denote the gearbox ratio and transmission efficiency.

The concise form of the equation of motion can be written as:

$$M\ddot{q} + C\dot{q} + K(q,t)q = f(q,t) \quad (1)$$

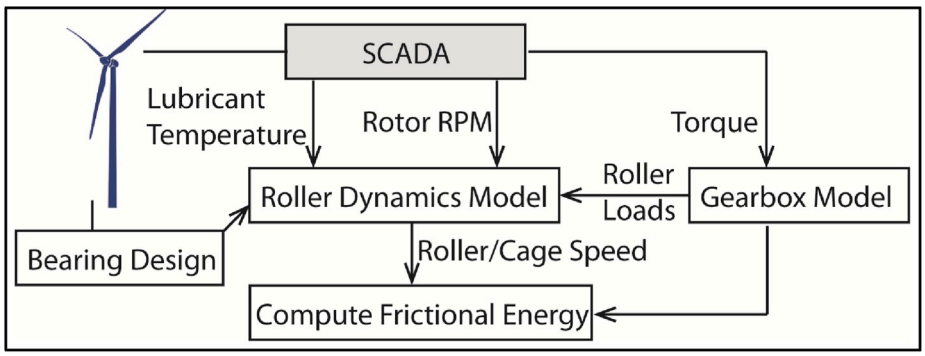

Fig. 1. Modeling steps for calculating frictional energy of individual bearings.

where M, C, K, and f denote the mass, damping, and stiffness matrices and the external loads and q denotes the displacements in two radial directions and one axial direction. In the model, bearing clearance is included to address its effects on bearing loads through piece-wise force-deflection functions [18]. The mass matrix, M, comprises the mass of the HSS and brake disk with the total mass of 668 kg. Modal damping of $\xi = 2\%$ is assumed in the simulation, where $C = 2\xi U^T diag\{\omega_n\}U$ and U and $diag\{\omega_n\}$ are the mode shapes and natural frequencies of the HSS. The stiffness matrix is based on the stiffness matrices of all three bearings in series connection, listed in Table 1. Finally, the gear mesh force is derived from T_h. Once the bearing loads are calculated, the roller load distribution is estimated using an analytic approach [19].

2.2. Roller dynamics model

With the calculated roller loads, shaft rotation speed, and lubricant temperature as the input, a dynamic bearing model calculates the frictional coefficient, bearing cage orbiting, and roller sliding speeds. This rolling element bearing model considers roller elasticity, roller dynamics, hydrodynamics of lubrication, lubricant temperature, and interactions between the lubricant and rollers. Modeling results compared well with direct measurement data on cage and roller speeds for cylindrical roller bearings [20].

2.3. Frictional energy

The bearing degradation that results in axial cracking is evaluated using the aforementioned accumulated frictional energy mechanism, given the calculated roller sliding speed and roller loads. The fundamental formula to calculate frictional energy for a single roller under sliding for a given period $[0, t]$ is:

$$E_j = \int_0^t \mu(\tau) Q_{ij}(\tau) \Delta V_{ij}(\tau) d\tau \tag{2}$$

where μ denotes the friction coefficient and Q_{ij} denotes normal force at the inner raceway of roller j. The sliding velocity ΔV_{ij} at the roller and inner-raceway contact surface equals:

$$\Delta V_{ij} = \frac{\pi}{60}\left(\omega_g B - \omega_c d_m - \omega_{rj} D\right) \tag{3}$$

where ω_g denotes generator rotational speed in rpm. ω_c and ω_{rj} denote the cage orbiting and roller, j, spinning speed, respectively. Parameters B, d_m, and D denote the bearing inner ring raceway, bearing pitch, and roller diameters.

For radially loaded bearings, only about half of the rollers are loaded. This loaded area is often called the bearing load zone. The rolling elements orbit with the cage, entering and leaving the loaded zone every orbit. To calculate the total frictional energy generated by all rolling elements in an orbit, Eq. (3) is reformulated to reflect the aforementioned cyclic and time-dependent loading for every roller. During normal production, the torque and speed spectra throughout the entire operation history are used as model inputs and divided into $N = 200$ bins. The estimated accumulated energy counts the accumulated ball-pass cycles $n_k, k = 1, \ldots, N$ with respect to the inner raceway ball-passing frequency under combined radial loads and sliding conditions for various wind speeds during the entire operation period, as shown in the following:

$$E(N) = \sum_{k=1}^{N} \left[\frac{n_k Z}{2\pi\omega_g} \int_0^{2\pi} \mu(k,\theta) C_{ij}(k,\theta) Q_{ij}(k,\theta) \Delta V_{ij}(k,\theta) d\theta \right] \tag{4}$$

where $C_{ij} = \frac{2b_{ij}Z}{\pi B}$ is the contact load factor that is defined as the ratio of the distance a single roller travels under continuous loading, b_{ij}, to the physical distance between two adjacent rollers. Z is the number of rollers. The parameter b_{ij} is estimated analytically as the length of contact ellipse in the circumferential direction based on Hertzian contact theory [19].

$$b_{ij} = 3.35 \times 10^{-3} \left[\frac{D(1-\gamma) Q_{ij}}{2L} \right]^{\frac{1}{2}} \tag{5}$$

where L denotes roller length and $\gamma = \frac{D}{d_m}$.

To analyze the reliability of gearbox bearings with respect to axial cracking, E is nondimensionalized by an estimate of the work done by bearing frictional force, μF_R, over the distance, $1440\pi\omega_g B$, that the rollers travel in 24 h as:

$$\widehat{E} = \frac{E}{1440\pi\mu\omega_g B F_R} \tag{6}$$

where F_R denotes the radial load on the bearing.

2.4. Variations in lubricant temperature and bearing clearance

The lubricant temperature and bearing clearance also have an important influence on the roller sliding velocity, and consequently, the accumulated frictional energy. The lubricant temperature is controlled by cooling and heating systems, whereas the bearing clearance is related to the bearing design, interference fit with the shaft, and the temperature of the bearing itself. These parameters also vary during turbine operation, just like the drivetrain load and speed, and must be accounted for when estimating frictional energy accumulation.

The measured lubricant temperature varies between 25^oC and 65^oC based on experiments conducted on a $1.5MW$ commercial wind turbine [4,21]. Fig. 3 shows the probability density function of the measured lubricant temperature and its Weibull fit analyzed in ReliaSoft [22]. The

Table 1
Stiffness matrix between HSS assembly including the bearings and gearbox housing.

Stiffness (N/m)	Axial	Radial	Tangential
Axial	890×10^6	12×10^6	1.5×10^6
Radial	12×10^6	5900×10^6	190×10^6
Tangential	1.5×10^6	190×10^6	2700×10^6

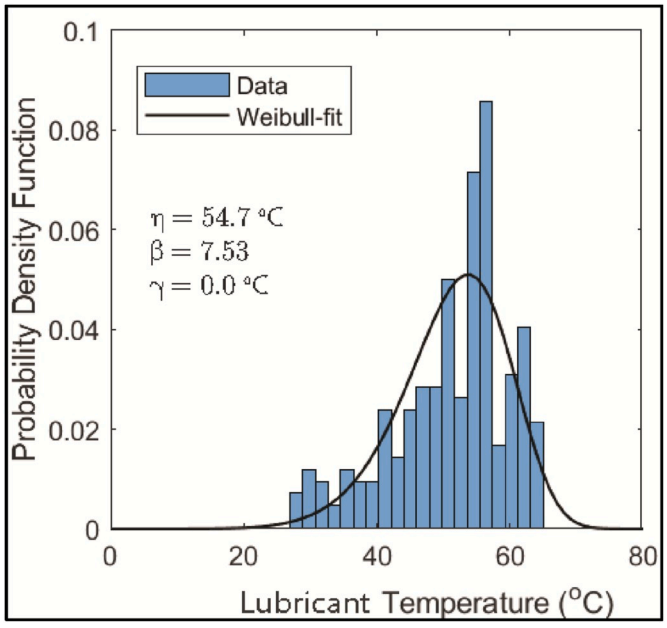

Fig. 3. Probability density function of the measured lubricant temperature.

expression of the probability density function of the three-parameter Weibull for the temperature spectrum is described as [23]:

$$\Psi(\mathrm{T}) = \frac{\beta}{\eta}\left(\frac{\mathrm{T}-\gamma}{\eta}\right)^{\beta-1} \exp\left[-\left(\frac{\mathrm{T}-\gamma}{\eta}\right)^{\beta}\right] \quad (7)$$

where β and γ denote the shape and location parameters, and η is the scale parameter of the Weibull-fitted spectrum. Weibull parameters of the lubricant temperature distribution are listed in Fig. 3, where the scale parameter of the lubricant temperature equals 54.7 °C.

Bearing clearance during operation can change significantly from its design value because of the interference fit with the shaft and differences in temperature between the rings and rollers. Because of the lack of direct experimental data, the variation of bearing operating clearance is estimated as [19]:

$$\Delta P_d = \Gamma[d_o(T_o - T_a) - d_i(T_i - T_a)] \quad (8)$$

where Γ denotes the coefficient of expansion of the bearing. Parameters T_o, T_i, and T_a denote the temperature at the bearing outer and inner rings, and ambient temperature, and d_o and d_i denote the outer and inner ring raceway diameters, respectively.

Fig. 4 shows the calculated frictional energy over the inner ring with various lubricant temperatures and bearing clearances. When the azimuth angle is less than 0, the rollers are outside the load zone and no meaningful energy is accumulated. When the azimuth angle is near 0, the rollers enter the load zone and accelerate. Roller sliding is greatest at this point while under low roller loads, resulting in the largest contribution to frictional energy. At the load zone center at an azimuth angle of $\frac{\pi}{2}$, the rollers are heavily loaded and experience the least amount of sliding, generating only small fraction of frictional energy. Once the rollers start to leave the load zone at an azimuth angle of π rad, they begin to decelerate, generating a moderate amount of frictional energy. As the lubricant temperature decreases, the amount of frictional energy increases because the lubricant is more viscous and causes more sliding. Fig. 4 also illustrates the frictional energy accumulation over the inner ring with C2, CN, and C3 bearing design clearances, ranging from 45 to 145 μm. The original design clearance is assumed to be 120 μm and 50 μm for RS and GS-in bearings, respectively. The bearing clearance has only a modest effect on the frictional energy in higher load cases, but can have a much greater effect in low load cases.

The proposed model considers these variations in lubricant temperature and bearing clearance during operation by integrating all temperatures. The probability density function of the lubricant temperature is discretized into 200 equally spaced bins. For a given power and rotor speed, 200 calculations of $\widehat{E}_k$ are simulated under various lubricant temperatures, as illustrated in Fig. 3, where k denotes the bin number. Then $\widehat{E}$ is computed as $\sum_k \Psi(T_k)\widehat{E}_k$, where $\Psi(T_k)$ is the probability density when the temperature is within bin k. Bearing clearance variation, ΔP_{dk}, is computed using Eq. (9) for every temperature bin, T_k.

2.5. Energy threshold

An essential step in the reliability analysis is determining $\widehat{E}^{\star}$, the frictional energy threshold. The amplitude of $E^{\star}$ has only been reported based on bench top testing of a roller sliding against three cylinders for a reference oil [8]. Thus, $\widehat{E}^{\star}$ needs to be determined for the gearbox high-speed bearings. The probability density function of $\widehat{E}^{\star}$ was estimated through Weibull-fitting of the calculated $\widehat{E}$ for the entire wind plant. The cumulative distribution function of the three-parameter Weibull can be derived as [23]:

$$\Phi(\widehat{E}) = 1 - \exp\left[-\left(\frac{\widehat{E}-\gamma}{\eta}\right)^{\beta}\right] \quad (9)$$

where η denotes the scale parameter. $\Phi(\widehat{E})$ indicates the percentage of the components among the entire wind plant that will have failed at a given $\widehat{E}$. For example, $\Phi(\widehat{E})$ equals 63.2% when $\widehat{E} = \eta + \gamma$.

Fig. 5 shows the Weibull cumulative distribution function of the accumulated frictional energy for the wind plant, calculated using aforementioned models. For the failed turbines, the accumulated energy was calculated during the mean time between failures. The entire operation period was considered for the healthy turbines. RS and GS-in bearings in both intermediate- and high-speed stages were considered in the analysis. The ReliaSoft Weibull fit [22] crosses the x-axis at a nonzero energy value (i.e., $\gamma > 0$). Based on the analysis, the scale parameter, η, equals 22.6. $\Phi(\widehat{E})$ equals 10% when $\widehat{E} = 1.97$. The goodness of Weibull fit equals 0.97, suggesting a very good fit despite the fact that the failure records cluster early in time. The coefficient of variation for this Weibull curve is estimated as 0.3 based on its β value [24]. Both the mean and variation of $\widehat{E}^{\star}$ are considered for the reliability analysis.

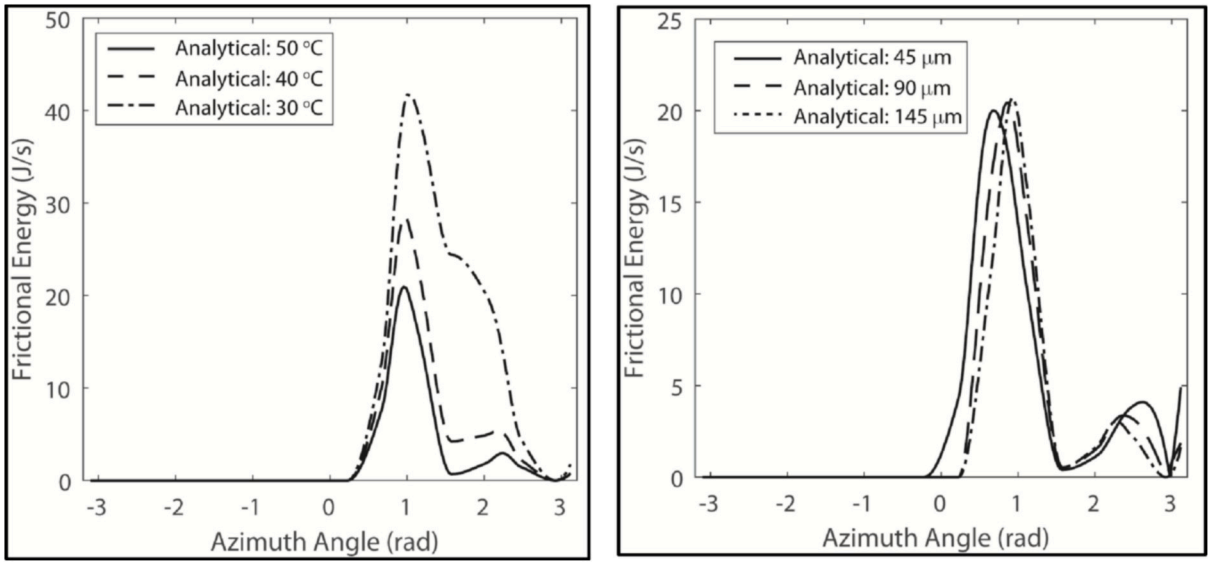

Fig. 4. Effect of (left) lubricant temperature and (right) bearing clearance on frictional energy.

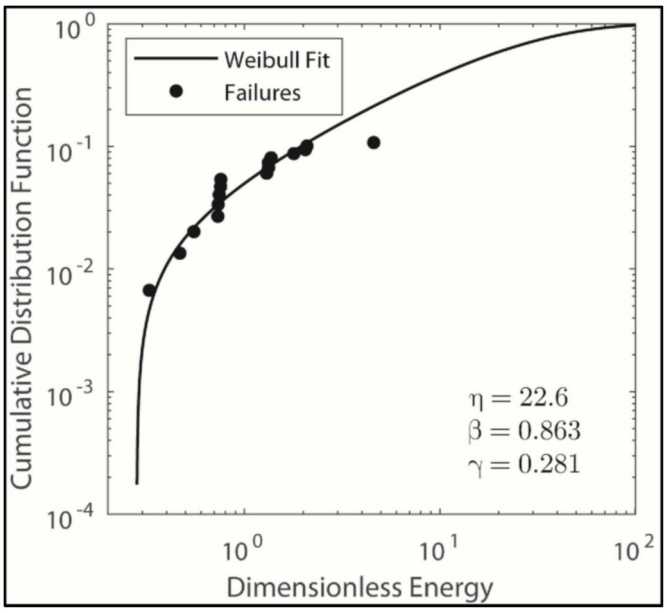

Fig. 5. The Weibull cumulative distribution function of dimensionless frictional energy accumulation.

2.6. Reliability analysis

The accumulation of frictional energy is an irreversible process that results in the formation of cracks and associated raceway spalling [7,8]. The probability of failure by axial cracking is estimated as bearing damage evolves toward the failure threshold, $\widehat{E}^{\star}$. A limit state function that separates the healthy and failure domains is defined as:

$$G = \widehat{E}^{\star} - \widehat{E}(N,t) \tag{10}$$

where $\widehat{E}^{\star}$ is the threshold beyond which axial cracking will occur and $\widehat{E}(N,t)$ is the accumulated frictional energy for the bearing, considering the variations of temperature and bearing clearance. When G is negative, failure is predicted.

The probability of failure is evaluated with the integral [25]:

$$P_f = P\{G<0\} = \int_{G(x)<0} f(x)dx \tag{11}$$

The parameter x is the vector that consists of all the considered variables. The function, $f(x)$, is the joint probability density function for these random variables. Direct evaluation of the probability integration can be difficult and time-consuming given the number of random variables and the nonlinearity in G.

FORM is an efficient way of estimating P_f [16,17] and is used in this study. This approach simplifies the integrand by transferring the random variables from their original random space, x, into standard normal space based on the knowledge that the cumulative distribution functions of the random variables remain the same before and after the transformation. Through searching the point on the integration boundary with the highest probability density, the distance from the origin to this most probable point, called the reliability index, R, is obtained. Therefore, the probability of failure can be estimated as [25]:

$$P_f = \Phi(-R) \tag{12}$$

where Φ is the cumulative distribution function of the standard normal distribution.

The limitations of the study include that it:

- relies on the degradation model for axial cracks, which was derived from benchtop experiments;
- focuses only on normal power production conditions averaged over 10-min periods. It does not investigate the potential effects of transient wind conditions and turbine events on roller sliding and bearing axial cracks; however, the frictional energy accumulated during transient events is much less than normal power production [26];
- addresses a limited number of uncertainties, including lubricant temperature, bearing clearance, and frictional energy accumulation. Uncertainties in bearing surface roughness, lubricant viscosity and additives, and material properties, as well as SCADA inputs, have not been considered;
- does not consider other data streams that could potentially augment reliability analysis, such as condition monitoring, because of the limited data availability.

3. Results and discussion

A total of forty-nine 1.5-*MW* wind turbines in a commercial wind power plant were analyzed to calculate the probability of failure of gearbox HSS bearings. The wind plant is located on a flat plain, but its northern border is close to a rugged valley. The dominant wind comes from the southwest. The secondary wind direction is from the northeast, across the valley mentioned earlier, which could cause wind turbulence. A majority of the time these turbines operate near either rated torque or very limited torque. The wind turbines all have three-stage gearboxes, with a transmission ratio of about 80, which are provided by multiple suppliers. Despite different gearbox manufacturers, cylindrical bearings are used in the intermediate- and high-speed stages. The data set includes 10 years of operational data and axial cracking failure records. In this study, a reliability analysis of this wind plant is performed assuming the plant has been operating for 20 years. Operation profiles of power and rotor speed from year 11–20 are assumed to be identical to those from year 1–10 to investigate the reliability of bearings during the gearbox design life.

3.1. Probability of failure analysis using frictional energy

Common maintenance practice typically treats the HSS and supporting bearings as one unit to save costs. When any part fails, the entire assembly is usually replaced. The fault tree analysis considers RS and GS-in bearings in a series relationship, resulting in:

$$\{P_f\}_{HSB} = 1 - (1 - \{P_f\}_{RS})(1 - \{P_f\}_{GS-in}) \tag{13}$$

Fig. 6 compares the P_f of the RS and GS-in bearings individually, and the high-speed-bearing (HSB) set together for all 49 wind turbines. The P_f for the individual bearings and the combined bearings monotonically increase with operating time, reaching 0.54, 0.63, and 0.83, respectively, after 20 years. The GS-in bearing has a slightly higher probability of failure than the RS bearing for this particular wind plant, which matches field observations. After 2.5 years, there were 9 failures out of 49 turbines on HSS bearings, equating to a failure percentage of 18%. As shown in Fig. 6, the probability of failure for the bearing set is about 20% after 2.5 years of operation, matching the previously mentioned calculation. Small differences in the P_f among these wind turbines are present; however, these differences in the P_f are insufficient to single out the unhealthy turbines from the entire population.

Fig. 7 compares the P_f of the HSB system for the individual turbines within the plant after 10 years and quantifies the small differences in P_f between turbines. The probability of failure ranges from 0.591 (wind plant row 2 and column 4) to 0.617 (wind plant row 1 and column 5). Quantifying P_f for each turbine can provide information for O&M decision-making. Furthermore, correlating the P_f of individual turbines with the wind plant layout may suggest the significance of terrain, wake,

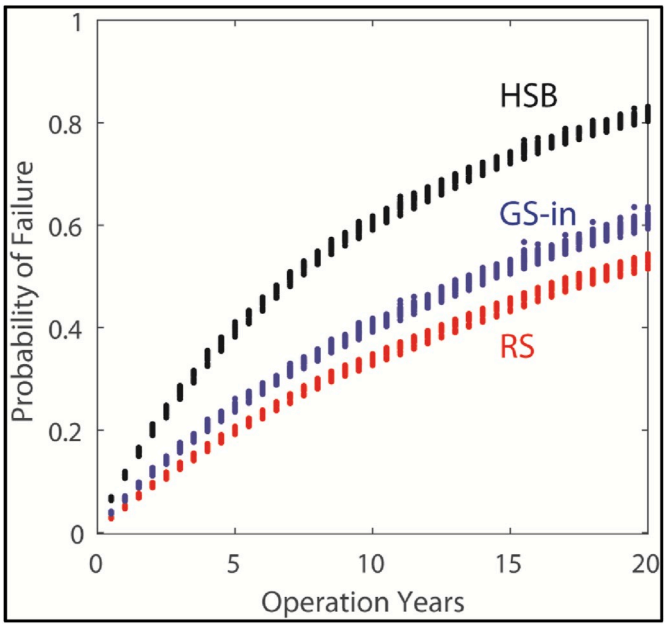

Fig. 6. RS, GS-in, and HSB system P_f based on frictional energy.

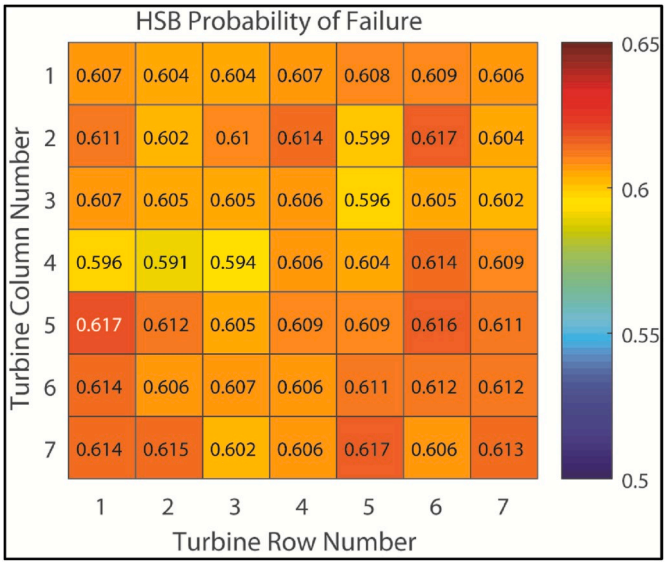

Fig. 7. HSB P_f of individual turbines within the plant after 10 years.

and other location-related factors on turbine health.

3.2. Probability of failure analysis using electrical energy generation

In addition to using frictional energy as a damage metric, electrical energy generation, *PH*, is also considered for comparison. It is a readily available measure of turbine usage but is the same for every bearing in the turbine. The process of calculating probability of failure based on electrical energy generation is the same as discussed previously, including determining the threshold, $PH^{\star}$, for the electrical energy using both SCADA and maintenance records, defining a limiting state function $G(PH) = PH^{\star} - PH$; and calculating the P_f using FORM. The probability density function of $PH^{\star}$ was determined by the Weibull fit of all of the healthy and failed wind turbines. Fig. 8 shows the cumulative distribution function from the Weibull fit. The scale parameter of $PH^{\star}$ is estimated as 1.62 *GWh*.

Fig. 9 shows the calculated P_f based on the measured energy

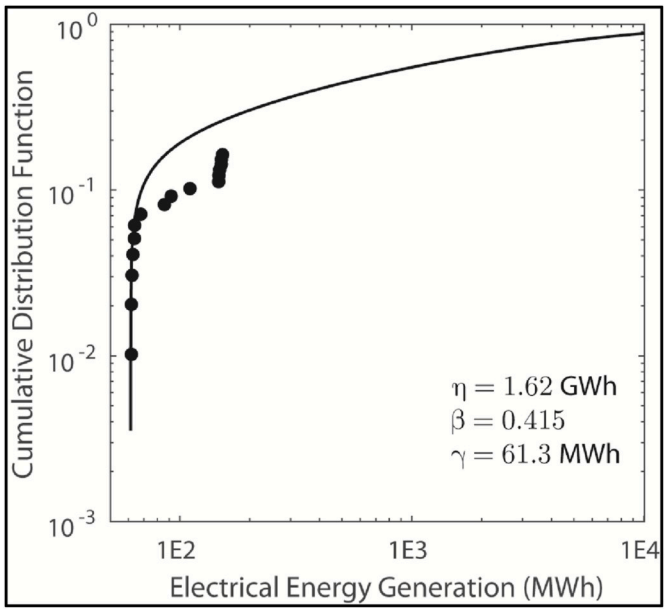

Fig. 8. Weibull cumulative distribution function for electrical energy generation.

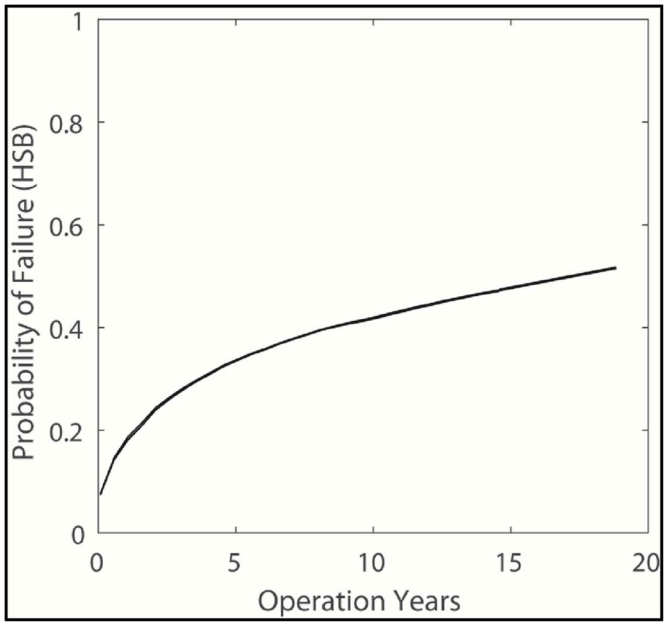

Fig. 9. HSB system P_f based on electrical energy generation.

generation for the same operation conditions as Fig. 6. Compared to Fig. 6, the P_f using energy generation shows the same trends and has a similar amplitude of 0.49 after 20 years (about 100 *MWh*). However, the P_f at low electrical energy has higher values than the frictional energy approach. Most importantly, the P_f of each of the 49 turbines is almost indistinguishable. Thus, P_f analyses using electrical energy generation cannot differentiate the axial-cracking risks among the turbines. Furthermore, a reliability assessment using electrical energy generation cannot assess the individual bearings. Despite these shortcomings, using electrical energy generation can provide a fast estimate of the risks of bearing axial cracking, but only at the wind plant level.

Both frictional energy and electrical energy generation reflect the usage of the turbine and result in highly correlated reliability predictions for the bearings. Even though electrical energy generation

cannot be used to quantify the reliability of individual bearings, it avoids the detailed calculations required of accumulated frictional energy.

3.3. Feature engineering analysis of damage metrics

The previous discussion of $\widehat{E}$ and PH suggests that studying damage metrics can be beneficial for further differentiating failure risks among wind turbines. Using the provided wind plant data, a feature engineering statistical analysis was conducted to investigate predictive features for the wind plant with a broader scope, including not only frictional energy and its constituent components, but also turbine siting metrics, the gearbox lubricant, and the gearbox manufacturer. The maximum, minimum, and mean values of roller loads, cage speed, roller deflections, sliding speed, roller speed, and frictional energy within every 10-min window are calculated for each turbine using the aforementioned mathematical models up to the point of failure. The distance from the nearby valley is considered as an additional feature that most likely introduces turbulence, as well as the distance to the nearest turbine as a potential source for wake influences.

The relationship between each of these features and the number of failures was assessed using box plots and quantified using a Wilcox test [27] for numerical features and Chi-squared test for the categorical variables (e.g., lubricant) [28]. The analysis is limited to a single turbine manufacturer and HSS bearing failures. Fig. 10 compares box plots of the averaged frictional energy and total electrical power generation over 10 years between failed and nonfailing high-speed bearing sets. The greater the difference between the healthy and failed distributions, the greater the chance that the feature is predictive. The electrical and frictional energy distributions for the healthy and failed wind turbines overlap significantly. Although there are observable differences in several features, the Wilcox test suggests that only the sliding speed maximum appears significantly correlated with failure when using the data subset analyzed here.

To assess the ability of combining multiple features to predict failures, multivariate model fitting using logistic regression and random forest models are explored. The considered features include terrain features, lubricant, frictional energy, roller loads, sliding speed, and electrical energy. The accuracy of each logistic or random forest model is studied by evaluating its ability to outperform a simple model that always chooses the most common class (i.e., no failure). The logistic regression and random forest model predict greater than 81% of accuracy, which is the baseline for the sample model. A random forest model that utilizes an ensemble tree classification modeling method performed the best and obtained 93% accuracy, with 97% sensitivity (true positive rate) and 75% specificity (true negative rate).

Despite the relatively small sample size and limited diversity of gearbox models, $\widehat{E}$ and its constituent components, combined with lubricant and terrain features, demonstrate some potential as prognostic precursors and damage metric for monitoring bearing axial cracking. More operational data and failure records from different wind plants and gearbox manufacturers are required to substantiate this finding. To fully understand the relationship between the constituent features and failure probability, questions about the ideal design of numerical experiments and analysis windowing of data must be addressed as well.

4. Conclusions

A methodology for reliability assessment and prognosis of wind turbine gearbox bearings is presented in this work. Unlike other reliability analysis approaches, the methodology uses a physics-domain model, SCADA data, and wind plant failure records to forecast the probability of failure of individual gearbox bearings in each wind turbine within the plant. It provides physical insight into the bearing failure mechanism and connects reliability to turbine design and wind plant operations. It can be used by turbine designers and plant operations to evaluate the effects of design and operations changes on bearing probability of failure to proactively prolong turbine life.

The methodology was applied to bearing axial cracking failures. Frictional energy accumulation and electrical power generation were considered as damage metrics. Only normal power production conditions were considered in the analysis because frictional energy accumulation is limited during transient turbine events. The reliability analysis using electrical power generation, although relatively simple, does not assess individual bearings like using frictional energy accumulation. Other damage metrics and physical drivers of bearing axial cracking may exist and could be explored using the established methodology.

The reliability analysis of 10-min-average SCADA data only showed small differences in the probability of failure for the wind turbines; however, these differences were insufficient to single out the failed turbines from the rest. A feature engineering analysis did show that the frictional energy and its constituent components, combined with

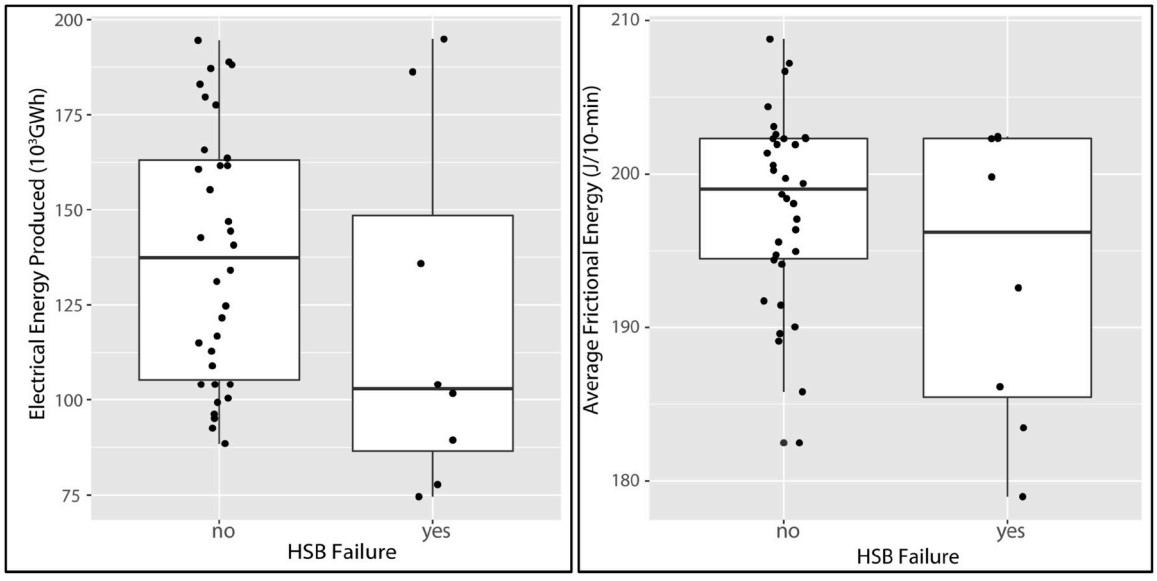

Fig. 10. Box plots of the (left) total electrical energy and (right) average frictional energy for healthy and failed HSBs. The horizontal line is the median and the box surrounds the interquartile range (25–75 percentile). The vertical line extends to the most extreme data points.

lubricant and terrain features, have some potential as a damage metric for monitoring bearing axial cracking. Further work is needed to refine the damage metric by incorporating additional prognosis precursors and examining a larger amount of high-resolution SCADA data and failure records.

Declaration of competing interest

None.

CRediT authorship contribution statement

Yi Guo: Conceptualization, Methodology, Validation, Investigation, Writing - original draft. **Shuangwen Sheng:** Conceptualization, Methodology, Investigation, Writing - review & editing. **Caleb Phillips:** Conceptualization, Methodology, Investigation, Writing - review & editing. **Jonathan Keller:** Conceptualization, Methodology, Investigation, Writing - review & editing. **Paul Veers:** Conceptualization, Methodology, Investigation, Writing - review & editing. **Lindy Williams:** Methodology, Investigation, Writing - review & editing.

Acknowledgements

This work was authored by the National Renewable Energy Laboratory, operated by Alliance for Sustainable Energy, LLC, for the U.S. Department of Energy (DOE) under Contract No. DE-AC36-08GO28308. Funding provided by the U.S. Department of Energy Office of Energy Efficiency and Renewable Energy Wind Energy Technologies Office. The views expressed in the article do not necessarily represent the views of the DOE or the U.S. Government. The U.S. Government retains and the publisher, by accepting the article for publication, acknowledges that the U.S. Government retains a nonexclusive, paid-up, irrevocable, worldwide license to publish or reproduce the published form of this work, or allow others to do so, for U.S. Government purposes. This work was made possible by the contributions from SKF GmbH under cooperative research and development agreement CRD-16-608, Flender Corporation under CRD-17-694, and wind power plant owner and operators that shared wind turbine SCADA data and maintenance records.

References

[1] Welte TM, Sperstad IB, Halvorsen-Weare EE, Netland, Nonås LM, Stålhane M. Operation and maintenance modeling. In: Anaya-Lara O, Tande JO, Uhlen K, Merz K, editors. Offshore wind energy technology. New Jersey: John Wiley & Sons Ltd.; 2018. p. 269–303. https://doi.org/10.1002/9781119097808.

[2] Sheng S, Keller J, Cotrell J, Greco A. Wind turbine drivetrain reliability collaborative workshop: a recap. Golden, CO: National Renewable Energy Laboratory; 2016. Report DOE/GO-102016-4878, https://www.nrel.gov/docs/fy16osti/66593.pdf.

[3] Sheng S. Gearbox reliability database: yesterday, today, and tomorrow, vol. 5. Golden, CO: National Renewable Energy Laboratory; 2014. NREL/PR-5000-63106, https://www.nrel.gov/docs/fy15osti/63106.pdf.

[4] Keller J, Lambert S. Gearbox instrumentation for the investigation of bearing axial cracking. Golden, CO: National Renewable Energy Laboratory; 2018. Technical report NREL/TP-5000-70639, https://www.nrel.gov/docs/fy18osti/70639.pdf.

[5] Evans MH. An updated review: white etching cracks (WECs) and axial cracks in wind turbine gearbox bearings. Mater Sci Technol 2016;32(11):1133–69. https://doi.org/10.1080/02670836.2015.1133022.

[6] Greco A, Sheng S, Keller J, Erdemir A. Material wear and fatigue in wind turbine systems. Wear 2013;302(1):1583–91. https://doi.org/10.1016/j.wear.2013.01.060.

[7] Gould B, Greco A. The influence of sliding and contact severity on the generation of white etching cracks. Tribol Lett 2015;60:29. https://doi.org/10.1007/s11249-015-0602-6.

[8] Gould B, Greco A. Investigating the process of white etching crack initiation in bearing steel. Tribol Lett 2016;62:26. https://doi.org/10.1007/s11249-016-0673-z.

[9] Sánchez-Silva M, Klutke G-A. Reliability and life-cycle analysis of deteriorating systems. first ed. Switzerland: Springer International Publishing; 2016. https://doi.org/10.1007/978-3-319-20946-3.

[10] Beconcini ML, Croce P, Marsili F, Muzzi M, Rosso E. Probabilistic reliability assessment of a heritage structure under horizontal loads. Probabilist Eng Mech 2016;45:198–211. https://doi.org/10.1016/j.probengmech.2016.01.001.

[11] Sheng S, Ryan O. Reliability of wind turbines. In: Letcher TM, editor. Wind energy engineering: a handbook for onshore and offshore wind turbines; 2017. p. 299–327. https://doi.org/10.1016/B978-0-12-809451-8.00015-1.

[12] Sheng S, Veers P. Wind turbine drivetrain condition monitoring - an overview. Proceeding of applied system health management conferences. 2011.

[13] Sheng S, Guo Y. A prognostics and health management framework for wind. Proceedings of ASME Turbo Expo. 2019.

[14] Lei Y, Li N, Guo L, Li N, Yan T, Lin J. Mechinery health prognostics: A systematic review from data acquisition to RUL prediction. Mech Syst Signal Process 2018;104:799–834. https://doi.org/10.1016/j.ymssp.2017.11.016.

[15] Okoh C, Roy R, Mehnen J, Redding L. Overview of remaining useful life prediction techniques in through-life engineering services. Procedia CIRP 2014;16:158–63. https://doi.org/10.1016/j.procir.2014.02.006.

[16] Veers P, Lange CH, Winterstein SR, Wilson TA. Theoretical Basis for FAROW: a computer analysis of the fatigue and reliability of wind turbine components. Albuquerque, NW: Sandia National Laboratories; 1994. Technical report SAND94-2459.

[17] Ditlevsen O, Madsen H. Structural reliability methods. first ed. Wiley; 1996.

[18] Guo Y, Parker RG. Dynamic analysis of planetary gears with bearing clearance. J Comput Nonlinear Dynam 2012;7(4):041002. https://doi.org/10.1115/1.4005929.

[19] Harris TA. Rolling bearing analysis. fourth ed. New York: John Wiley & Sons; 2001.

[20] Guo Y, Keller J. Validation of combined analytical methods to predict slip in cylindrical roller bearings. Tribol Int 2020;148:106347. https://doi.org/10.1016/j.triboint.2020.106347.

[21] Keller J, Guo Y, Sethuraman L. Uptower investigation of main and high-speed-shaft bearing reliability. Golden, CO: National Renewable Energy Laboratory; 2019. Technical report NREL/TP-5000-71529.

[22] ReliaSoft [Computer software], https://www.reliasoft.com/. [Accessed 31 March 2020].

[23] Mann NR, Schafer RE, Ray E, Singpurwalla ND. Methods for statistical analysis of reliability and life data. Wiley series in probability and mathematical statistics: applied probability and statistics. first ed. New York: John Wiley & Sons; 1974.

[24] International Electrotechnical Commission (IEC) 61649. 2008 -Weibull analysis, technical report. International Electrotechnical Commission; 2018. https://webstore.iec.ch/publication/5698.

[25] Pipinato A. Innovative bridge design handbook: construction, rehabilitation and maintenance. Butterworth-Heinemann; 2015.

[26] Guo Y, Keller J, Sheng S. Quantification of roller sliding energy in wind turbine gearbox high-speed shaft bearings. Golden, CO: National Renewable Energy Laboratory; 2014. NREL/PR-5000-73320.

[27] Bauer DF. Constructing confidence sets using rank statistics. J Am Stat Assoc 1972;67(339):687–90. https://doi.org/10.1080/01621459.1972.10481279.

[28] Agresti A. An introduction to categorical data analysis. Wiley; 2018.